EFDA–JET–CP(10)06/31

D. Zarzoso, M.N.A. Beurskens, L. Frassinetti, T. Eich, E. Joffrin, A. Loarte, G. Maddison, F.G. Rimini, G. Saibene, E.R. Solano, H. Thomsen and JET EFDA contributors

ELM Size Analysis in JET Advanced Tokamak and Hybrid Scenarios

ELM Size Analysis in JET Advanced Tokamak and Hybrid Scenarios

D. Zarzoso[1], M.N.A. Beurskens[2], L. Frassinetti[3], T. Eich[4], E. Joffrin[1,8], A. Loarte[5], G. Maddison[2], F.G. Rimini[8], G. Saibene[7], E.R. Solano[6], H. Thomsen[4] and JET EFDA contributors*

JET-EFDA, Culham Science Centre, OX14 3DB, Abingdon, UK

[1]Association EURATOM-CEA IRMF, 13108 St Paul-lez-Durance, France
[2]EURATOM-CCFE Fusion Association, Culham Science Centre, OX14 3DB, Abingdon, OXON, UK
[3]Association EURATOM-VR, Department of Physics, SCI, KTH, SE-10691 Stockholm, Sweden
[4]Max-Planck-Institut für Plasmaphysik, EURATOM-Assoziation, D-85748 Garching, Germany
[5]ITER organization, F-13067 Saint-Paul-lez-Durance Cedex, France
[6]Laboratorio Nacional de Fusion, Asociacion EURATOM-CIEMAT, Madrid, Spain
[7]Fusion for Energy Joint Undertaking, 08019 Barcelona, Spain
[3]EFDA-CSU, Culham Science Centre, OX14 3DB, Abingdon, OXON, UK
** See annex of F. Romanelli et al, "Overview of JET Results",*
(Proc. 22 nd IAEA Fusion Energy Conference, Geneva, Switzerland (2008)).

Preprint of Paper to be submitted for publication in Proceedings of the 37th EPS Conference on Plasma Physics, Dublin, Ireland.
(21st June 2010 - 25th June 2010)

ABSTRACT.

ELM size analysis for standard ELMy H-mode plasmas (baseline scenario) has been the subject of multi machine studies. In the projection from current devices towards ITER baseline scenarios, the empirically found negative correlation of ELM losses normalized to the pedestal stored energy ($\Delta W_{ELM}/W_{ped}$) with pedestal neoclassical collisionality (ν^*_{ped}) would imply ELM losses of 20% of the pedestal energy at the ITER relevant ν^*_{ped}. In addition to the baseline scenarios, Advanced Tokamak (AT) and hybrid scenarios allowing an improved core confinement are under investigation in existing devices. This paper sets out to characterise the normalised losses of type I ELMs in the range $0.05 < \nu^*_{ped} < 0.7$ for a data base of 26 baseline, 13 AT and 56 hybrid plasmas.

The pedestal energy has been calculated as [1]

$$W_{ped} = \frac{3}{2} k_B \left(n_{e,ped} T_{e,ped} + n_{i,ped} T_{i,ped}\right) V_{plasma} \tag{1}$$

where kB is the Boltzmann constant and the electron density and temperature at the top of the pedestal are calculated with a modified *tanh* fit performed on the new high resolution Thomson scattering (HRTS) data. The ion density is calculated as $n_{i,ped} = n_{e,ped} \frac{7 - Z_{eff}}{6}$ under the assumption that carbon is the only impurity present in the tokamak and the ion pedestal temperature is calculated as $T_{i,ped} = \left.\frac{T_i}{T_e}\right|_{r \quad 0.8a} T_{e,ped}$, with T_i taken from the core Charge exXchange (CX). ELM losses are measured by W_{dia}, which depends only on external magnetic measurements of the poloidal field and the plasma toroidal flux. It reflects only the perpendicular component of the plasma pressure and includes the effect of thermal and fast particles.

The energy drop is obtained assuming that the plasma energy increases linearly after the ELM, which means that a linear regression on can be performed before and after the pedestal collapse and the difference of the values yields the ELM loss. This method removes difficult to measure effects around the ELM crash, possibly due to eddy currents induced in the vacuum vessel and rapid plasma movements on a millisecond timescale which can impact diamagnetic measurements. An alternative method is to calculate the ELM energy loss from the pre- and post-ELM electron kinetic profiles from the HRTS system as described in [3].

All the discharges analysed in this paper exhibit regular type I ELMs of steady frequency and no large compound ELMs. In addition, the time windows of interest have been chosen outside of any detectable core MHD activity (such as neoclassical tearing modes) by diamagnetic measurements. Figure 1 shows an example of W_{dia} signal averaged over many ELMs and synchronised to the ELM crash time for the hybrid Pulse No77922 - with ELM frequency of 17.3Hz, $I_p = 1.7$MA, $B_t = 2.3$T. Figure 2 illustrates the measured frequency of the ELM energy loss for the same hybrid discharge.

Analysis of the dependence of the ELM losses on the ν^*_{ped} (as defined in [1]) for 26 baseline discharges is carried out. The database covers the following range in dimensionless parameters:

$\beta_N(1.8 < \beta_N < 3.6)$, q_{95} $(2.5 < q_{95} < 3.8)$, ρ^*_{ped} $(0.002 < \rho^*_{ped} < 0.005)$ and triangularity ($\delta \approx 0.25$ and $\delta \approx 0.4$). In Figure 3 circles represent the values when W_{dia} is used for the ELM losses calculation and black points represent the JET baseline discharges analysed in [1] (these data have been taken directly from this reference). Each point represents one single discharge and the values are averaged over a time window of typically several seconds during a stead phase in the discharge. The general negative correlation is observed in agreement with [1], corroborating the consistency of our data analysis. The correlation $\rho\Delta W_{ELM}, Y = \frac{\sigma^2_{\Delta W_{ELM}}, Y}{\sigma_{\Delta W_{ELM}}, \sigma Y}$ of the ELM losses with dimensionless parameters $Y \in \{\nu^*_{ped}, q_{95}, \delta\}$nis greater than 0.8 for each.

When we analyse the AT and hybrid discharges, with a similar range of variation of ν^*_{ped}, we find a weaker correlation coefficient of < 0.5 between the normalized losses and collisionality. This is illustrated in Fig.4. In general, for high triangularity, the losses are larger for AT and hybrid discharges than for baseline plasmas. For low triangularity, hybrid and baseline plasmas exhibit similar ELM energy losses. We have isolated nine discharges from gas-scan sessions and observed that a modification of gas-fuelling may result in a strong modification of the ELM energy losses without considerably affecting the collisionality. This seems to be in agreement with [2], where it was shown that the gas-fuelling strongly affect the ELM characteristics. Table 1 gives a summary of some of the characteristics of each discharge. For these nine discharges, the dependence of the normalized ELM losses on collisionality is shown in Fig.5. Further analysis on the ELM penetration has been carried out. We have observed that, for baseline plasmas and $\nu^*_{ped} \geq 0.2$, the ELM affected area extends up to 20% of the minor radius, whereas for un-fuelled AT and hybrid plasmas this region is larger (up to 50% of the minor radius). However, the ELM penetration seems to be modified by increasing the gasrate. Indeed, Fig.6 shows two hybrid discharges (left) and two AT discharges (right) with collisionalities between 0.1 and 0.3. We observe how the ELM affected area can be strongly reduced with a small change in collisionality, resulting in a decrease of the ELM energy losses. This is consistent with the results published in [3].

CONCLUSION

It has been found that, although the ν^*_{ped} ordering is well reproduced for JET baseline scenarios, for AT and hybrid discharges no clear correlation exists. A possible dependence of the ELM affected area on the gas-fuelling rate has been observed, which may explain the high dispersion observed in Fig.4.

ACKNOWLEDGEMENTS

This work was supported by EURATOM and carried out within the framework of the European Fusion Development Agreement. The views and opinions expressed herein do not necessarily reflect those of the European Commission.

REFERENCES

[1]. A. Loarte et al., Plasma Physics and Controlled Fusion **45** (2003)

[2]. M.N.A. Beurskens et al., Nuclear Fusion **48** (2008)

[3]. Y. Sarazin et al., Plasma Physics and Controlled Fusion **44** (2002)

Pulse No:	B_t (T)	I_p (MA)	P_{NBI} (MW)	Gas-rate (10^{21} e/s)
75957	2.7	1.8	19.9	–
75960	2.7	1.8	20.0	6.0
75959	2.7	1.8	19.6	7.0
75954	2.0	1.7	18.4	–
75964	2.0	1.7	18.3	7.51
75963	2.0	1.7	18.3	7.62
75962	2.0	1.7	18.3	10.64
76746	2.0	1.7	18.6	10.64
76748	2.0	1.7	14	25

Table 1: Summary of some of the characteristics of the AT and hybrid gas-scan discharges used in this paper

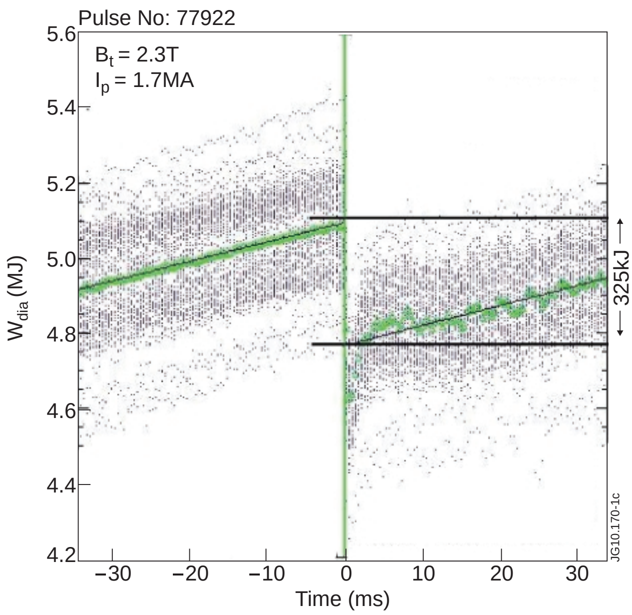

Figure 1: plasma energy evolution for a single JET hybrid discharge. Green lines show the computed average at a given time and the ELM energy drop is inferred from the distance between the horizontal lines.

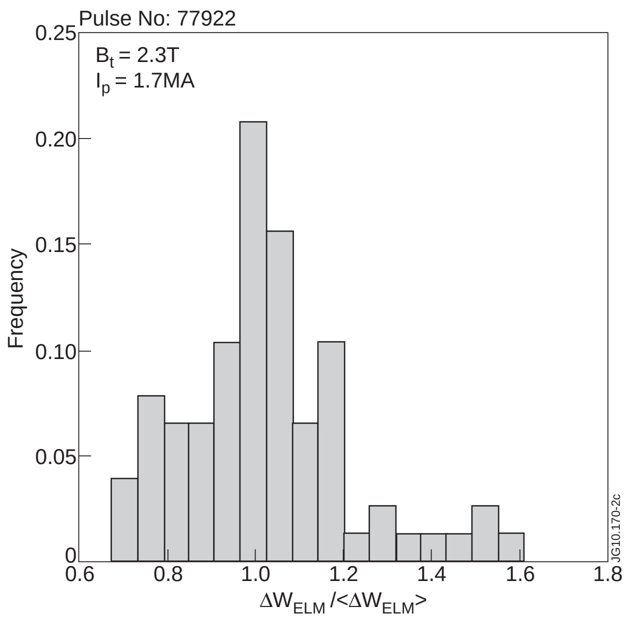

Figure 2: Histogram of the frequency of the ELM energy loss for a single JET hybrid discharge. A sample of 90 ELMs has been used with a standard deviation of 20%.

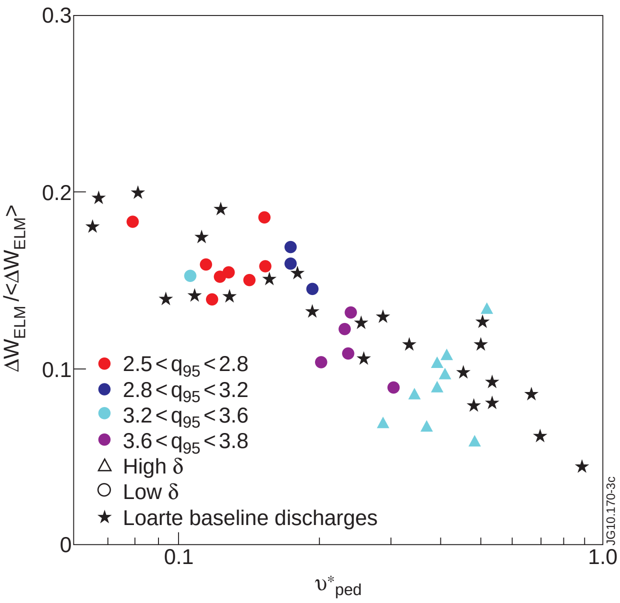

Figure 3: Normalizad ELM energy losses versus pedestal plasma collisionality for new JET baseline discharges (circles). Comparison is made with the discharges analized in [1] (black points).

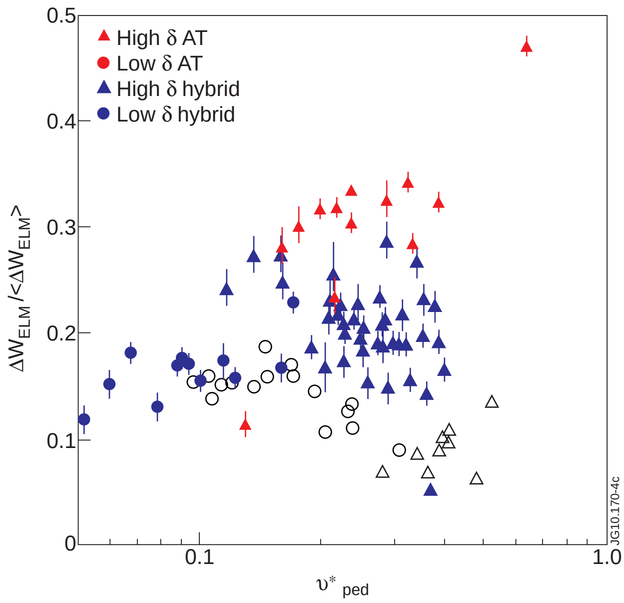

Figure 4: normalized ELM energy losses versus pedestal plasma collisionality for JET AT and hybrid discharges.

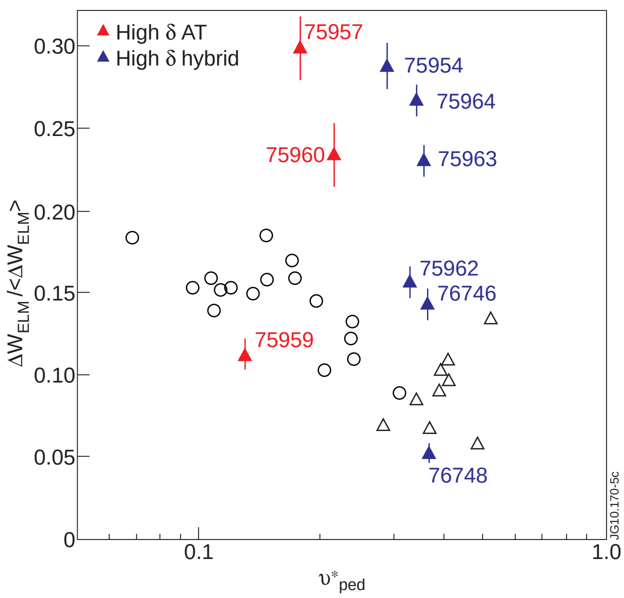

Figure 5: ELM losses versus collisionality for JET AT and hybrid gas-scan discharges.

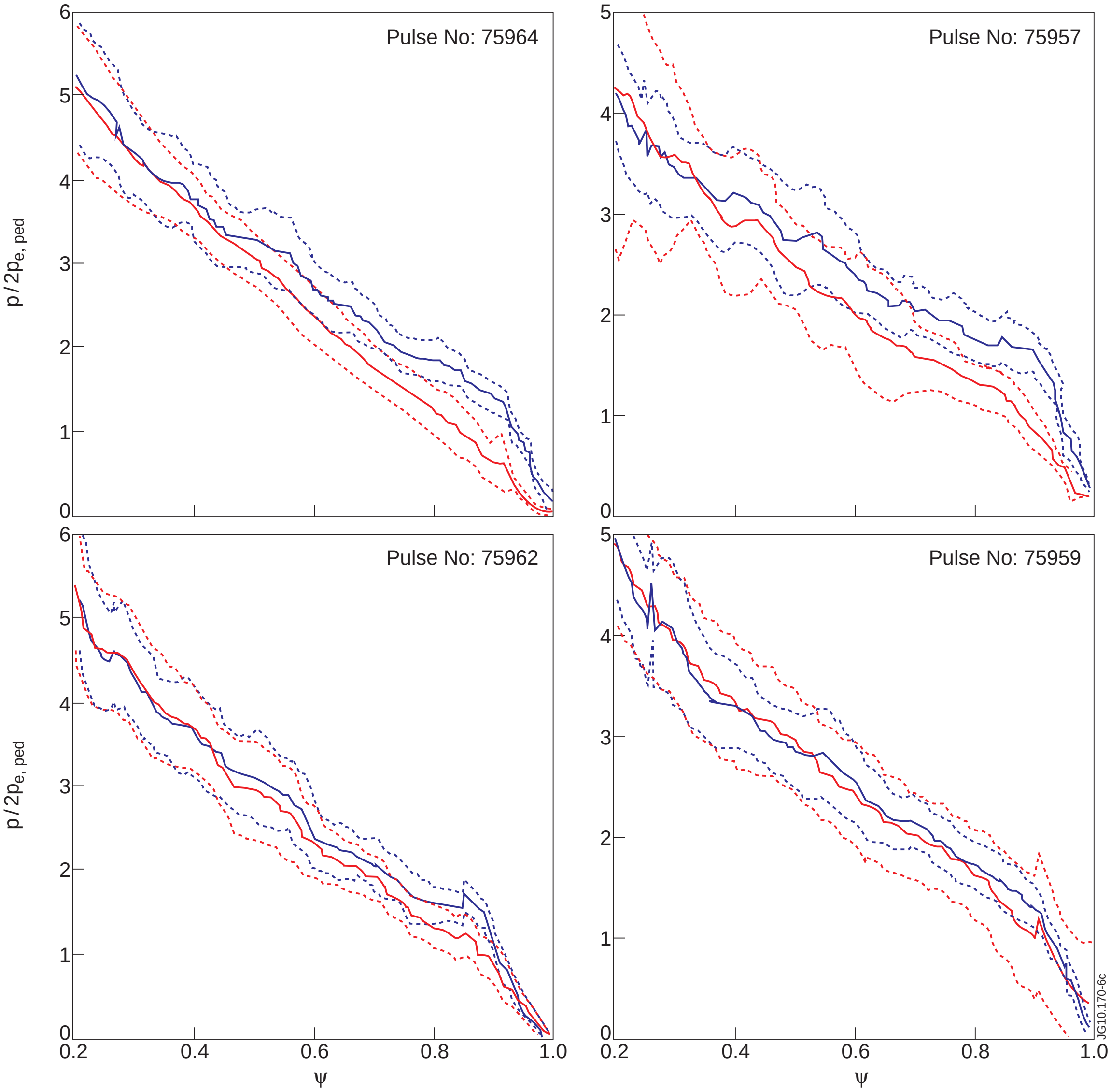

Figure 6: Pre-ELM (blue lines) and post-ELM (red lines) normalized pressure profiles reconstructed from HRTS and CX. Dashed lines represent the standard deviation region. Solid lines represent the averaged profiles.